

Primary energy spectra of cosmic rays selected by mass groups in the knee region

H. Ulrich¹, T. Antoni², W.D. Apel², F. Badea³, K. Bekk², A. Bercuci², H. Blümer^{2,1}, E. Bollmann², H. Bozdog³, I.M. Brancus³, C. Büttner², A. Chilingarian⁴, K. Daumiller¹, P. Doll², J. Engler², F. Feßler², H.J. Gils², R. Glasstetter¹, R. Haeusler², W. Hafemann², A. Haungs², D. Heck², J.R. Hörandel¹, T. Holst², A. Iwan^{1,5}, K-H. Kampert^{2,1}, J. Kempa^{5,+}, H.O. Klages², J. Knapp^{1,¶}, G. Maier², H.J. Mathes², H.J. Mayer², J. Milke², M. Müller², R. Obenland², J. Oehlschläger², M. Petcu³, H. Rebel², M. Risse², M. Roth², H. Schieler², J. Scholz², T. Thouw², B. Vulpescu³, J.H. Weber¹, J. Wentz², J. Wochele², and J. Zabierowski⁶

¹Institut für Experimentelle Kernphysik, University of Karlsruhe, 76021 Karlsruhe, Germany

²Institut für Kernphysik, Forschungszentrum Karlsruhe, 76021 Karlsruhe, Germany

³National Institute of Physics and Nuclear Engineering, 7690 Bucharest, Romania

⁴Cosmic Ray Division, Yerevan Physics Institute, Yerevan 36, Armenia

⁵Department of Experimental Physics, University of Lodz, 90236 Lodz, Poland

⁶Soltan Institute for Nuclear Studies, 90950 Lodz, Poland

⁺now at: Warsaw University of Technology, 09-400 Plock, Poland

[¶]now at: University of Leeds, Leeds LS2 9JT, U.K.

Abstract. The KASCADE experiment measures the electron and muon number of extensive air showers in the knee region with high precision. From these data shower size spectra for electrons and muons are constructed. An analysis is presented in which electron and muon size spectra in three different zenith angle bins are analysed simultaneously. With a four component assumption for the mass composition of primary cosmic rays (hydrogen, helium, carbon and iron) and using unfolding methods taking into account shower fluctuations and experimental effects energy spectra of these mass groups in the range between 10^{15} and 10^{17} eV are reconstructed. Each energy spectrum shows a steepening of the index of the resulting power law with a knee-like structure. The positions of the individual knees suggest a rigidity dependence.

array contains four liquid scintillation counters to measure the electromagnetic part of the shower. The outer stations contain only two of these detectors but additionally below an iron-lead absorber plastic scintillators to measure muons. Using the information of these detectors it is possible to reconstruct the location of the shower core, the direction of the shower and using the NKG formula the total number of electrons N_e and the so called *truncated muon number* N_μ^{tr} . The latter one is the number of muons inside a ring around the shower core with an inner radius of 40 m and outer radius of 200 m. Simulations have shown that this quantity is more robust against systematical reconstruction errors than the total muon number. During the reconstruction the contributions of accompanying particles in each detector are taken into account. A detailed description of the setup and the reconstruction procedure can be found in (Doll et al., 1990) and (Antoni et al., 2001).

In the present analysis the electron and truncated muon number are used. The data were taken from May 1998 until December 1999 and correspond to a total number of about 35 Mio. showers. The aim of the analysis is to determine the primary energy spectra of different mass groups by analysing the shower size spectra of N_e and N_μ^{tr} in intervals of the zenith angle simultaneously.

1 Introduction

The KASCADE experiment (Klages et al., 1997) located at the site of the Forschungszentrum Karlsruhe, Germany at an altitude of 110 m a.s.l. measures various observables of an extensive air shower especially in the *knee*-region (10^{14} – 10^{17} eV). It consists of three major detector components: the scintillation detector array, the muon tracking detector and the central detector complex.

The field array covers an area of $200 \times 200 \text{ m}^2$ and consists of 252 detector stations for the detection of the electron and muon component. The stations in the inner part of the

2 Outline of the Analysis

To reconstruct the primary energy spectrum by means of the shower size spectra (electron size or/and muon size spectra) it is useful to apply the relation between the measured flux

of the shower size $dJ/d\lg N$ and the primary energy flux $dJ(\lg E)/d\lg E$ for individual types of primary particles. This relation is a Fredholm integral equation of 1st kind:

$$\frac{dJ_A}{d\lg N} = \int_{-\infty}^{+\infty} \frac{dJ_A(\lg E)}{d\lg E} p_A(\lg N | \lg E) d\lg E \quad (1)$$

$p_A(\lg N | \lg E)$ is the probability for a primary particle of type A with energy $\lg E$ to be reconstructed as an air shower with shower size $\lg N$. This *kernel function* p_A factorizes into three parts: the shower fluctuations $s_A(\lg N^t | \lg E)$, the efficiency $\epsilon_A(\lg N^t)$ for the triggering of the measurement, and the reconstruction accuracy $r_A(\lg N | \lg N^t)$. We assume that the probability for a trigger only depends on the particular type of particles under investigation (electrons or muons).

$$p_A(\lg N | \lg E) = \int_{-\infty}^{+\infty} k_A(\lg N^t) d\lg N^t \quad (2)$$

with

$$k_A(\lg N^t) = r_A(\lg N | \lg N^t) \epsilon_A(\lg N^t) s_A(\lg N^t | \lg E) \quad (3)$$

N^t is the true shower size since normally the reconstructed shower size N does not coincide with the true one.

Looking at real data integration over an interval of zenith angle must be taken into account since all the functions depend on the zenith angle via the atmospheric thickness. For the sake of simplicity this is omitted in the formulas above but is a key point in the analysis presented below.

In the present analysis four primary components were assumed: hydrogen, helium, carbon and iron. So the general equation in this case reads

$$\frac{dJ}{d\lg N} = \sum_{A=1} \int_{-\infty}^{+\infty} \frac{dJ_A(\lg E)}{d\lg E} p_A(d\lg N | d\lg E) d\lg E \quad (4)$$

A powerful tool to solve Fredholm integral equations of 1st kind is in general known as *unfolding*. There exist several different unfolding methods each one appropriate to special problems. For the method chosen the first step is the formulation of the integral equation as a matrix equation. This will be done in the following only for one primary particle type A . Again, integration over the zenith angle is not explicitly mentioned as above.

The data are arranged in a vector with dimension n . The number of events in each bin i is y_i . Now one is searching for the corresponding histogram or vector of the energy spectrum with dimension m . These vector elements are labeled as x_j^A . Defining the matrix elements R_{ij}^A of the *response matrix* \mathbf{R}_A

$$R_{ij}^A = \frac{\int_{bin\ i} d\lg N \int_{bin\ j} d\lg E \frac{dJ_A(\lg E)}{d\lg E} p_A(\lg N | \lg E)}{\int_{bin\ j} d\lg E \frac{dJ_A(\lg E)}{d\lg E}} \quad (5)$$

one obtains

$$y_i = \sum_{j=1}^m R_{ij}^A x_j^A \quad (6)$$

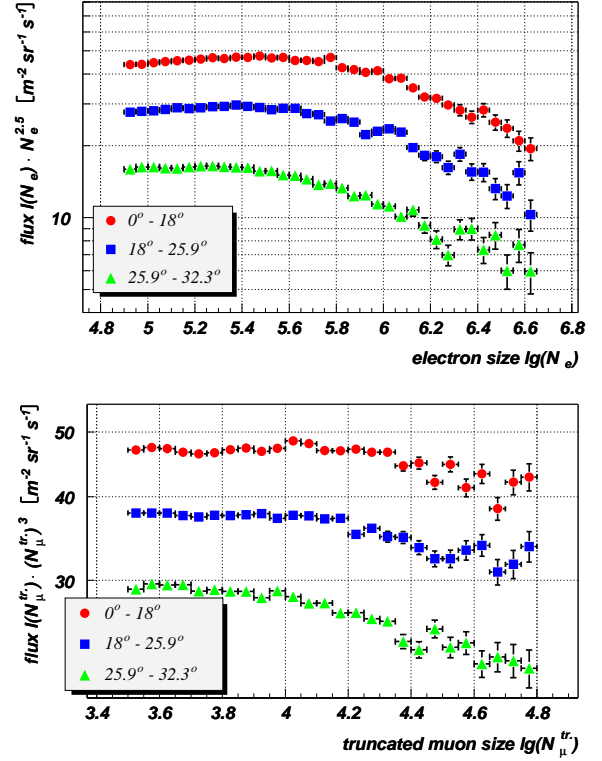


Fig. 1. Electron size spectra (upper plot) and truncated muon size spectra (lower plot) in intervals of zenith angle. The data have not been corrected for reconstruction accuracy.

The elements R_{ij}^A depend on the unknown distribution. However, for sufficiently narrow bins the result will become insensitive to the exact form of $J_A(\lg E)$. For practical purposes it is sufficient in the most cases to use a best guess of the unknown distribution. Of course, the result of the unfolding procedure must be checked for any systematical bias due to the binwidth and this simplification.

The data in the analysis consist of N_e and N_μ^{tr} spectra in three zenith angle bins: $0^\circ < \vartheta < 18^\circ$, $18^\circ < \vartheta < 25.9^\circ$ and $25.9^\circ < \vartheta < 32.3^\circ$. They are displayed in fig. 1. The lower histogram borders were chosen in a way that the muon and electron size spectra are not affected by the trigger threshold, so that they can be treated as independent. The data vector \mathbf{y} consists of 6 spectra. The response matrices \mathbf{R}_A of the four components are arranged in one response matrix \mathbf{R} consisting of 24 submatrices, the vector \mathbf{x} represents the four unknown energy spectra.

The unfolding method chosen is the *Gold-algorithm* (Gold, 1964). This is an iterative scheme which computes the next solution using the one obtained before. The algorithm produces only non-negative solutions and tries to minimize the χ^2 functional. Defining the error matrix \mathbf{C} of the data and the modified response matrix \mathbf{G} with $\mathbf{G} = \mathbf{C} \mathbf{R}$ the iterative scheme can be written as

$$\mathbf{x}^{k+1} = \mathbf{x}^k \frac{(\mathbf{G}^T \mathbf{G} \mathbf{G}^T) \mathbf{C} \mathbf{y}}{(\mathbf{G}^T \mathbf{G} \mathbf{G}^T \mathbf{G}) \mathbf{x}^k} \quad (7)$$

where x^{k+1} is the estimate in the $k + 1$ -iteration, x^k the estimate in the k th iteration and y is the data vector. Products of the matrix G and its transpose G^T are used instead of G to fulfill the requirements of the algorithm. The number of allowed iterations can be chosen to give an acceptable small value of χ^2 or to be dependent on the convergence rate (e.g. if the value of χ^2 is not changing any more).

3 Calculating the Response Matrix

In order to obtain the response matrices R_A one usually simulates Monte Carlo events at least in the same order of magnitude as have been measured. When dealing with extensive air showers this is not possible. To overcome this problem of limited statistics the distributions were parametrized and the matrix elements calculated separately. The air showers were simulated using the CORSIKA package (Heck et al., 1998) version 5.623 with the QGSJet model (Kalmykov, N.N. and Ostapchenko, S.S., 1993) with activated thinning option. By using the thinning option it is possible to generate high energy air showers with high statistics. All simulations were performed using an appropriate zenith angle distribution. The distributions $s(\lg N_e | \lg E)$ and $s(\lg N_\mu^{tr.} | \lg E)$ can be very well described by the product of an error function and an inverse error function with the same mean:

$$s(\lg N_{e,\mu} | \lg E) \propto \text{erf}(\lg N_0, \sigma_1)(1 - \text{erf}(\lg(N_0, \sigma_2))) \quad (8)$$

For the determination of the efficiencies and reconstruction accuracy a second sample of full simulated EAS was generated which corresponds to a continuous E^{-2} spectrum. These showers were used as input for the KASCADE detector simulation based on the GEANT package (GEANT, 1993). The showers were analysed with the standard KASCADE analysis software. The efficiencies can be well described using an error function, the reconstruction accuracies are well described by a gaussian. All the relevant parameters are parametrized as functions of primary energy or true shower size. This procedure was performed for each of the four assumed primary particle types with the same number of simulated showers.

4 Results

After applying the unfolding algorithm to the experimental data one obtains the four energy spectra displayed in fig.2. Each of the spectra shows a knee like structure shifted to higher energy with increasing mass. The knee in the total energy spectrum at about 5 PeV (dependent on the definition of the knee) is caused mostly by the steepening of the spectra of the light components. The quoted vertical error bars display only the statistical errors. The horizontal error bars display the systematic uncertainties in the energy assignment. For reasons of a clear presentation an estimate of the systematical errors is only displayed for the iron spectrum. These systematical errors include the uncertainties in the used parametriza-

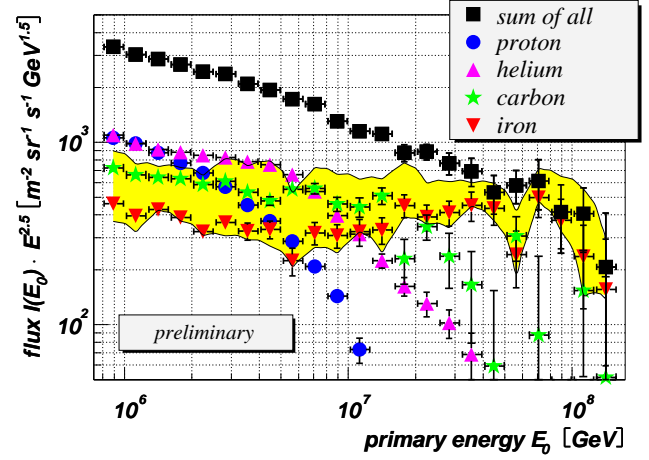


Fig. 2. Result of the unfolding procedure. The vertical error bars are statistic errors, the horizontal reflects the uncertainty in the energy assignment. The shaded yellow band displays the estimated size of systematical errors in the case of iron.

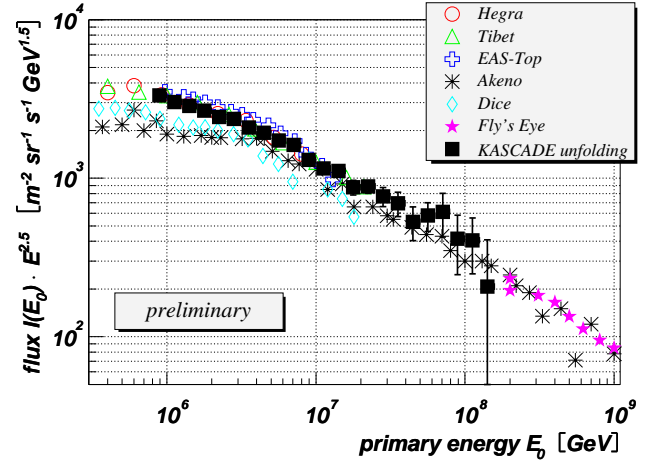


Fig. 3. Comparison of the total energy spectrum with spectra reported by other experiments. Error bars are only statistical ones.

tions and their parameters, the uncertainties in the used energy spectra for the calculation of the matrix elements, and the systematics introduced by the unfolding algorithm. The latter is mainly crosstalk between the individual components i.e. due to the limited resolution power of the algorithm. The systematical errors are largest for the iron component. The total energy spectrum is hardly affected by these systematical errors.

In figure 3 the obtained total energy spectrum is compared with the results of other experiments (taken from Hörandel et al. (1999)). A very good agreement with the data of Tibet and Hegera is found. Also there's a excellent agreement when analysing the data with nonparametric methods, e.g. neural networks (Roth et al., 2001).

In fig.2 the spectra of the lighter components appear to be steeper below the knee as compared to the heavier ones. Also the starting position of the steepening of the spectrum

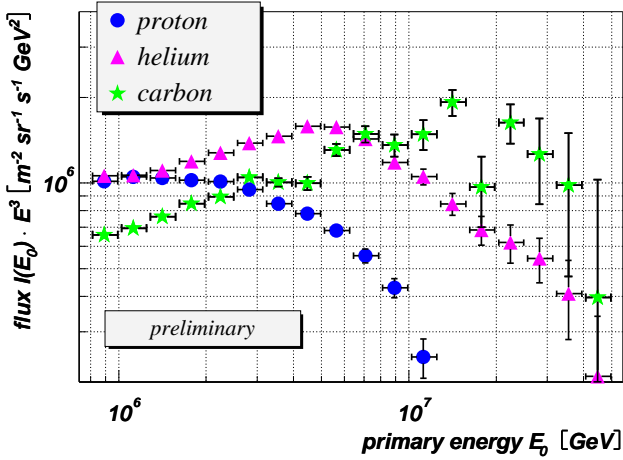


Fig. 4. The flux spectra of proton, helium and carbon primaries between 1 PeV and 10 PeV. The differential flux is scaled with E^3 .

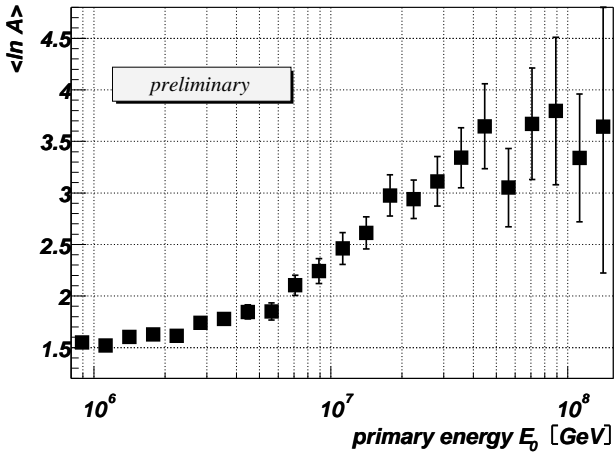


Fig. 5. The mean logarithmic mass versus primary energy. Only statistical errors are displayed.

is shifted to higher energies for the heavier components. To investigate these dependencies the spectra of hydrogen, helium and carbon are displayed in figure 4 in the energy range between 1 PeV and 10 PeV. The differential energy flux is multiplied by E^3 . Again the systematical errors are omitted for reasons of a clearer representation.

The helium and carbon spectra show a relatively sharp knee whereas the proton knee appears very smooth. As can be seen the index of the power law describing the individual energy spectra below the knee is steeper for proton than for helium, and flatter for carbon than for helium. Looking at the starting positions of the index change (e.g. defined as the first point below the extrapolation from the points to the left) one finds a factor of 2-3 between proton and helium and a factor of ≈ 3 between helium and carbon. The factor between iron and proton is around 20, but less well defined due to the larger statistical uncertainties. The data thus suggest a rigidity dependence of the individual knees. Since systematical errors are still large this has to be treated with caution

and kept in mind when drawing quantitative conclusions. Regarding these results it is on the other hand unlikely that the knee position is dependent on the atomic mass A .

As a result of the spectra in fig. 2 the chemical composition of the primary cosmic rays becomes heavier with increasing energy. This is also reflected in the mean logarithmic mass $\langle \ln A \rangle$ displayed as a function of the primary energy in figure 5. It slowly starts to increase at about 2.5 PeV from a constant value up to about 45 PeV when $\langle \ln A \rangle$ starts to saturate.

5 Conclusions

Using unfolding algorithms the energy spectra of four mass groups (proton, helium, carbon and iron) of the primary cosmic radiation have been reconstructed. As input the shower size spectra of electrons and muons in different angular intervals were used and analysed simultaneously. Each of the obtained spectra shows a knee-like feature. The results suggest that the position of the individual knees depends on the nuclear charge Z . Since the systematical uncertainties are still relatively large further investigations will focus on this point. All the results were obtained using CORSIKA with the QGSJet model and have to be seen in this context. Future investigation will also be carried out using other hadronic interaction models.

Acknowledgements. The KASCADE experiment is supported by Forschungszentrum Karlsruhe and by collaborative WTZ projects in the frame of the scientific-technical cooperation between Germany and Romania (RUM 97/014), Poland (POL 99/005) and Armenia (ARM 98/002). The Polish group (Soltan Institute and University of Lodz) acknowledges the support by the Polish State Committee for Scientific Research (grant No. 5 P03B 133 20).

References

- Antoni, T. et al., KASCADE Collaboration, *Astrop. Physics* 14, 245–260, 2001.
- Doll, P. et al., KASCADE Collaboration, Kernforschungszentrum Karlsruhe, Report KfK-4648, 1990.
- GEANT, CERN Program Library Long Writeup W5013, CERN, Geneva, 1993.
- Gold, R., Argonne National Laboratory Report ANL-6984, Argonne, 1964.
- Heck, D. et al., Forschungszentrum Karlsruhe, Report FZKA 6019, 1998.
- Hörandel, J. et al., KASCADE Collaboration, Proc. 26th ICRC, Salt Lake City, HE 2.2.41, 1999.
- Kalmykov, N.N. and Ostapchenko, S.S., *Yad. Fiz.* 56, 105, 1993.
- Klages, H.O. et al., KASCADE Collaboration, *Nucl. Phys. B (Proc. Suppl.)* 52B, 92–102, 1997.
- Roth, M. et al., KASCADE Collaboration, Proc. 27th ICRC, Hamburg, 2001.